

Dynamic Core–Shell Structures in Two-State Models of Neutral Water-Soluble Polymers

N. Yoshinaga

Department of Physics, Graduate School of Science, Kyoto University, Kyoto 606-8502, Japan

D. J. Bicout

Institut Laue-Langevin, 6 rue Jules Horowitz, B.P. 156, 38042 Grenoble, France, and Biomathematics and Epidemiology, ENVL-TIMC, B.P. 83, 69280 Marcy l'Etoile, France

E. I. Kats

Laue-Langevin Institute, F-38042, Grenoble, France, and L. D. Landau Institute for Theoretical Physics, RAS, 117940 GSP-1, Moscow, Russia

A. Halperin*

Structures et Propriétés d'Architectures Moléculaires, UMR 5819 (CEA, CNRS, UJF), DRFMC/SPRAM, CEA-Grenoble, 38054 Grenoble cedex 9, France

Received September 23, 2006; Revised Manuscript Received January 10, 2007

ABSTRACT: Monte Carlo simulation of annealed copolymers of solvophobic/solvophilic monomers show collapsed globular states having dynamic core–shell structures. In these, the core is mostly solvophobic while the core boundary contains an excess of solvophilic monomers. This two-state model, where each monomer undergoes interconversion between solvophobic and solvophilic state, is a minimal version of models of neutral water-soluble polymers such as PEO. The reduced surface tension of such core–shell structures suggests an explanation of the stability of PNIPAM globules as observed in the experiments of Wang et al. [Wang, X.; Qiu, X.; Wu, C. *Macromolecules* **1998**, *31*, 2972]. The statistics of the monomeric states along the chain vary with the degree of chain swelling. They differ from those of quenched copolymers designed to create water-soluble globules though both systems involve a core–shell structure.

I. Introduction

Discussions of neutral homopolymer collapse typically invoke a Flory free energy.^{1–3} Within this picture all monomers are identical, and only the second virial coefficient can change sign. The corresponding phase diagram exhibits only an upper critical solution temperature (UCST). This description is generally appropriate for collapse in nonaqueous solvents. In the experimentally accessible concentration range collapse is concomitant with aggregation leading to precipitation. The collapse of neutral water-soluble polymers (NWSP) in aqueous media involves additional ingredients associated with the occurrence of a lower critical solution temperature (LCST). Of particular interest are the experimental observation concerning three NWSP exhibiting a LCST: poly(*N*-isopropylacrylamide) (PNIPAM), poly(*N*-vinylcaprolactam) (PVCL), and poly(vinyl methyl ether) (PVME).⁴ In aqueous solutions of these polymers collapse can occur without precipitation. Two scenarios were reported. In one the collapsed chains form stable aggregates of finite size, “mesoglobules”.^{4,5} In the second, single chains form thermodynamically stable solution of collapsed globules.^{4,6–9} Importantly, the current rationalization of these effects invokes models and mechanisms that apply also to neutral homopolymers in nonaqueous solvents.⁴ In the following we discuss a distinctive mechanism operative in NWSP in aqueous media as described by “two-state models”.^{10–19} Within these models the monomers are assumed to interconvert between two states: a hydrophilic state (P) that is favored at low temperatures and a hydrophobic (H) state that is preferred at high temperatures. Thus far, the theory of the collapse of two-state polymers received little

attention.^{14,18,20–25} In the following we present simulation results, supplemented by simple theory, regarding the structure of two-state globules and its consequences. The simulation addresses directly two questions concerning the collapse of a single, annealed, two-state polymer: First, what is the spatial distribution of the P and H monomers within the globule? Second, what is the effect of the collapse on the PH sequence along the chain? As we shall discuss, collapsed globules of such “two-state polymers” exhibit a dynamic core–shell structure comprising of an inner hydrophobic core surrounded by a hydrophilic shell. While the PH distribution in the swollen state is random, the PH sequence in the core–shell globules exhibits correlations. As we shall argue on the basis of Lifshitz–Grosberg theory of collapse,²⁶ the surface tension of such dynamic core–shell structures is lower in comparison with the corresponding one-state polymer globules. In turn, this affects the phase diagram in that it contributes to the stabilization of dilute solutions of globules against precipitation.¹ This effect, which is not accounted for in phase diagrams obtained from Flory-type free energies, is of relevance to the interpretation of the experimental observations of thermodynamically stable collapsed globules of PNIPAM as reported by Wu et al.^{6–9} It is important to note that the annealed core–shell globules we discuss, where the P and H monomers interconvert, differ from quenched core–shell structures^{4,9,27} obtained by chemical modifications of the chains that lead to a fixed HP sequence.

The two-state models of NWSP were mostly developed for aqueous solutions of poly(ethylene oxide) (PEO).^{10–19} They were largely utilized to analyze the phase behavior of aqueous

PEO solutions using a modified form of the Flory free energy that allows for the interconversion between the two states. In particular, they rationalize the closed loop phase boundary, with both upper and lower critical solution temperatures, that is thought to characterize NWSP.²⁸ Two observations are of interest. First, the various models differ with respect to the precise identification of the states: polar vs apolar, hydrated vs nonhydrated, or clustered vs nonclustered. Direct experimental evidence concerning the interconverting states is yet to emerge. However, some form of interconversion between hydrophobic and hydrophilic states is a common key ingredient. Second, these models do not incorporate the detailed chemical structure of the polymer. Rather, they introduce phenomenological parameters fixed by comparison with experimental results concerning a particular polymer. The two-state models may thus be used to describe NWSP of different structures provided they exhibit similar phase behavior. Because of these two observations there is an interest in studying generic features of such models. With this in mind we performed off-lattice Monte Carlo simulations of the collapse behavior for a minimal model of a single two-state polymer. There is no explicit solvent in the simulation where the monomers undergo a unimolecular HP interconversion. The monomers states are modeled as Lennard-Jones particles with an identical collision diameter but different interaction parameters. Our model is thus closest to the one proposed by Karlström.¹¹

Since our results concern single-chain behavior, they are directly relevant for the interpretation of the results of Wu et al. However, the mechanism invoked may also contribute to the stabilization of “mesoglobules” incorporating a number of chains. From a theory perspective, these results complement earlier works in this area. Most simulations of NWSP focus on PEO and involve all-atom simulation of the *swollen* polymer and the surrounding water molecules.^{29–31} Relatively little attention was devoted to the effect of the two-state hypothesis on the collapse behavior of NWSP chains. Simulations concerning this aspect utilized minimal models and focused on the nature of the collapse, suggesting a first-order phase transition.^{14,22} Our approach is similar in spirit to the one adopted by Jeppesen and Kremer¹⁴ in that it incorporates two-state monomers but avoids an all-atom simulation. It concerns however a different aspect of the problem. Instead of investigating the nature of the transition, it focuses on the structure of the collapsed globule. A full analytical discussion of the collapse of two-state polymers is currently unavailable. We will comment on the existing models^{18,20,21,23–25} and their relevance to our results in the discussion. The dynamic core–shell globules we discuss are also of interest in view of recent results concerning the design of “protein-like” copolymers of hydrophobic and hydrophilic/polar monomers reported in series of papers by Khokhlov et al.^{27,32} This design aims to obtain HP sequences such that the core of the collapsed globules will be hydrophobic while its exterior will be occupied by hydrophilic P monomers. Its outcome imitates the amino acid residues sequence of natural proteins yielding guidelines for the synthesis of polymers capable of forming dense, water-soluble globules. The design procedure involves the *in silico* generation of collapsed homopolymer globules and transforming the H monomers at the surface to P monomers. Once generated, they permit to characterize the statistics of PH sequences. As we shall discuss, such PH sequences are reminiscent of the ones generated by the two-state models. They differ however in two respects. First, the PH ratio in the protein-like sequences was constrained to unity while in the two-state polymers it is determined by

thermodynamic equilibrium. Second, the “protein-like” sequences are quenched and reflect the requirement that all exterior monomers are hydrophilic. In two-state polymers the sequence is annealed, and only a fraction of the exterior monomers is hydrophilic. As we shall see, these differences lead indeed to distinguishable sequence statistics in the two cases.

The experimental studies of the collapse behavior of PNIPAM motivate our work, and we thus discuss them in some detail. Wu et al. investigated the collapse of high molecular weight (MW) PNIPAM in extremely dilute solutions.^{6–9} The chains' size diminishes with increasing temperature in the range $20\text{ }^{\circ}\text{C} \leq T \leq 36\text{ }^{\circ}\text{C}$. For chains having MW of $\approx 1.3 \times 10^7$, corresponding to polymerization degree of $N \approx 1.15 \times 10^5$, a collapse transition was observed in the range $30.6\text{--}32.4\text{ }^{\circ}\text{C}$. Importantly, for the concentration studied, $[\text{PNIPAM}] = 6.7 \times 10^{-7}\text{ g/mL}$, the collapsed chains did not exhibit aggregation for 33 h, thus suggesting thermodynamically stable solution.^{6,7} Furthermore, the density of the collapsed globule was found to be 0.34 g/cm^3 as compared to $\approx 0.4\text{ g/cm}^3$ predicted for a space-filling model. This collapse behavior was also found for somewhat shorter chains, $N \approx 9.56 \times 10^4$ and $N \approx 1.07 \times 10^5$, studied at a higher concentration of $[\text{PNIPAM}] = 5 \times 10^{-6}\text{ g/mL}$. However, in this last case an onset of aggregation was observed for $T > 32\text{ }^{\circ}\text{C}$.⁸

The experimental evidence suggesting that dilute solutions of collapsed PNIPAM globules are thermodynamically stable is difficult to reconcile with the theory of “normal” homopolymers whose monomers exist in a single state. In this framework one expects aggregation and phase separation to take place at much lower concentrations compared to the ones studied by Wu et al. The equilibrium between a dense phase and a dilute solution of collapsed globules is specified by the equality of the chemical potential of individual chains in the two phases,¹ i.e., $\mu_{\text{dilute}} = \mu_{\text{dilute}}^0 + kT \ln(c_{\text{dilute}}/N)$ and $\mu_{\text{dense}} = \mu_{\text{dense}}^0 + kT \ln(c_{\text{dense}}/N)$. Here k is Boltzmann constant, T is temperature, and c_{dilute} and c_{dense} specify the number concentration of monomers in the two phases while μ_{dilute}^0 and μ_{dense}^0 are the corresponding standard chemical potentials. The volume free energy contributions to the two μ^0 are identical because one may consider the dense phase as the interior of an infinite collapsed globule. The difference between the two μ^0 is due the surface free energy of the globules $\mu_{\text{dilute}}^0 - \mu_{\text{dense}}^0 = F_{\text{surface}}$. In the strong segregation limit, when the thickness of the interface is of order of a monomer size a , the surface tension of dense globules can be estimated by $\gamma \approx kT/a^2$. This estimate is justified for dense globules, in the vicinity of the space-filling limit, as observed by Wu et al.^{6–8} Since the radius of the globule is $R \approx N^{1/3}a$, the surface free energy γR^2 is $F_{\text{surface}} \approx kTN^{2/3}$, thus leading to

$$\frac{c_{\text{dilute}}}{c_{\text{dense}}} \approx \exp(-N^{2/3}) \quad (1)$$

In turn, this suggests aggregation leading to phase separation at $[\text{PNIPAM}] \ll 6.7 \times 10^{-7}\text{ g/mL}$. This disagreement between theory and experiment arises because of the assumption that PNIPAM is a “simple” homopolymer. In this case, a collapsed globule in the vicinity of its close packing density can be viewed as droplet of a single component fluid having a sharp interface, of width $\sim a$, thus suggesting $\gamma \approx kT/a^2$. However, to obtain phase diagram exhibiting a LCST, as is the case for PNIPAM, it is necessary to invoke two-state models of the type proposed for PEO. Accordingly, the dense fluid interior comprises of a binary mixture rather than a single component. When core–shell structures develop, the width of the PH “interface” replaces

a in the estimate of γ , thus leading to a lower value. Three additional observations merit discussion at this point. First, Wu et al. proposed that the collapse involves a “molten globule” state, involving a dense core decorated by small nondraining loops, reminiscent of the fringed globule considered by Lifshits and Grosberg.²⁶ This hypothesis provides a possible rationalization for the observed ratio of the radius of gyration, R_g , and the hydrodynamic radius, R_h . In particular, the observation of R_g/R_h is smaller than that predicted for a uniform hard sphere. Such a state is difficult to justify within the single-state theory of polymer collapse when considering high-density globules, suggesting the strong segregation limit. However, such scenarios may be envisioned within two-state models. Second, the insufficiency of the collapse models of “one-state” homopolymers for the description of the collapse of PNIPAM was noted by Wu et al. from a different point of view. In particular, these models accounted well for the chain swelling in the low T , corresponding to coils, but failed to describe the quantitative features of the high T regime, corresponding to the collapsed globules. Finally, as noted earlier, most models of polymer collapse are based on a Flory free energy of homopolymers with monomers having a single state. These lead to a virial expansion where only the second virial coefficient can change sign upon varying T . In contrast, the introduction of two-state models allows for change of sign of higher order virial coefficients signaled also by concentration dependence of the Flory χ parameter.³³ Note that collapse models that are inapplicable to PNIPAM are however well suited to describe the collapse of polystyrene in cyclohexane, where precipitation occurs only upon cooling, as studied by Chu et al.³⁴

The remainder of the article is organized as follows: The simulation model is outlined in section II. The spatial distribution of P and H monomers in different swelling states is analyzed in section III, demonstrating the occurrence of dynamic core-shell structure for dense globules. The statistics of the PH sequences are discussed in section IV. In particular, we compare the correlations in sequences corresponding to swollen chains and dynamic core-shell structures in the annealed case to those obtained for the quenched PH sequences giving rise to protein-like core-shell structures as reported by Khokhlov et al. Complementary theoretical considerations are presented in section V. These are comprised of two parts. One aims to relate fraction of P monomers to the simulation parameters by considering the PH equilibrium when the PH sequences are weakly sensitive to the precise backbone configurations. In highly swollen chains the P fraction is well approximated by considering a unimolecular reaction in an ideal PH solution. In the dense globule the equilibrium is modified by monomer-monomer interactions as described via binary PH mixture model utilizing the Bragg-Williams approximation. The second part concerns the surface tension of dynamic core-shell structures of two-state polymers as compared to the surface tension of one-state polymer. This argument is based on general features of the Lifshitz-Grosberg²⁶ theory of collapse. In the Discussion we will comment on earlier theoretical studies and their relationship to our work. In addition, we briefly outline the evidence for vertical phase separation in PNIPAM brushes, of interest as a related form of core-shell structure tractable to the two-state character of PNIPAM.

II. Simulation Model

The polymers are modeled as freely jointed chain of Lennard-Jones (LJ) particles following Baumgartner.³⁵ The monomers within this bead-spring model interact via a LJ potential

$$V_{LJ} = 4\epsilon \sum_{ij} \left[\left(\frac{a}{r_{ij}} \right)^{12} - \left(\frac{a}{r_{ij}} \right)^6 \right] \quad (2)$$

where \mathbf{r}_i is the three-dimensional coordinate of the i th monomer and $r_{ij} = |\mathbf{r}_i - \mathbf{r}_j|$ is the distance between monomers i and j . Here ϵ specifies the depth of the potential at the minimum in $r_{ij} = 2^{1/6}a$, and a , the collision diameter, is the separation for which $V_{LJ} = 0$. The monomers are thus modeled as soft spheres with a steeply decaying attractive branch for $r_{ij} \geq a$. The monomers exist in two interconverting states, P and H. It is thus necessary to specify three LJ potentials, corresponding to the interactions between PP, HH, and PH, involving six parameters. In the following all three potentials are characterized by the same a . For brevity, we will thus express all distances in units of a . The three remaining parameters, $\epsilon_{PP}kT$, $\epsilon_{PH}kT$, and $\epsilon_{HH}kT$, determine the strength of attraction between the PP, PH, and HH monomers. In addition, $\Delta\epsilon kT$ specifies the difference in chemical potential between noninteracting H and P monomers, $\Delta\mu^0$, as given by eq 8. Here we will introduce $\Delta\epsilon$ via the transition probabilities among noninteracting monomers as discussed below. We have chosen to fix $\epsilon_{PH} = \epsilon_{PP} = 0.20$ so as minimize the attractive component between the PH and HH pairs which thus experience mostly excluded volume interaction. The chain configurations are explored for different values of ϵ_{HH} and $\Delta\epsilon$. All monomer pairs except nearest neighbors interact via V_{LJ} potentials. Nearest-neighbor monomers along the chain are constrained to $0.7 \leq (\mathbf{r}_{i+1} - \mathbf{r}_i)^2 \leq 2.0$. Separations outside this range incur an infinite energy penalty, thus ensuring connectivity. At each Monte Carlo step we shift the position of every monomer and update its HP state. The initial HP distribution is random, and the transition probabilities at each step are

$$\begin{aligned} p(H \rightarrow P) &= p(P \rightarrow P) = \frac{1}{2} \exp(-\Delta\epsilon) \\ p(P \rightarrow H) &= p(H \rightarrow H) = 1 - \frac{1}{2} \exp(-\Delta\epsilon) \end{aligned} \quad (3)$$

where $\Delta\epsilon$ can vary between $-\ln 2$ and ∞ , corresponding to $0 \leq p(H \rightarrow P) \leq 1$. For the case of noninteracting monomers the equilibrium fraction of H monomers, x_0 , is determined by detailed balance, $x_0 p(H \rightarrow P) = (1 - x_0) p(P \rightarrow H)$, leading to

$$\frac{x_0}{1 - x_0} = \frac{p(H \rightarrow P)}{p(P \rightarrow H)} \equiv K^0 \quad (4)$$

Tuning $\Delta\epsilon$ in the range $-\ln 2$ and ∞ thus results in $0 \leq x_0 \leq 1$. The Monte Carlo procedure utilizes the Metropolis method. Thus, a change of energy ΔE , reflecting the LJ interactions and the “connectivity” contribution, is calculated for each updated monomer state. When $\Delta E \leq 0$, the update is accepted, while for $\Delta E > 0$ it is retained with the probability $\exp(-\Delta E/kT)$. The simulations involved 5 million Monte Carlo steps (MCs), where each step comprises updates and trials for each of the N monomers. The equilibration time of the chain dimensions and of the PH statistics are somewhat different. For $N = 500$ steady state is attained after $\approx 10^4$ MC steps, and ≈ 300 chain configurations were thus retained for analysis.

III. Simulation Results: Radial Distribution of States

Of the various regimes generated by variation of ϵ_{HH} and $\Delta\epsilon$ we focus on the good and poor solvent behavior, with swollen and collapsed configurations, as evident from the plots of the radius of gyration R_g vs N . For $\epsilon_{HH} = 1.0$ these exhibit

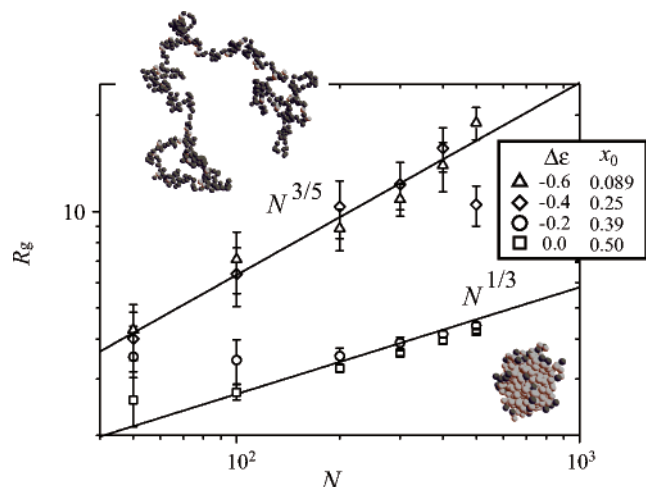


Figure 1. Plots of $\log R_g$ vs $\log N$ for $\epsilon_{HH} = 1.0$ and various $\Delta\epsilon$ or x_0 values. The insets depict snapshots of swollen and collapsed globules where the P monomers are colored in dark gray.

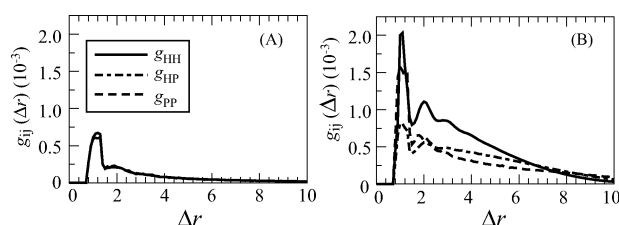


Figure 2. Pair correlation functions $g_{ij}(\Delta r)$ of PH two-state polymer with $N = 500$ and $\epsilon_{HH} = 1.0$ for (A) swollen ($\Delta\epsilon = -0.6$ or $x_0 = 0.089$) and (B) collapsed core-shell ($\Delta\epsilon = -0.2$ or $x_0 = 0.39$) configurations.

respectively $N^{3/5}$ and $N^{1/3}$ scaling (Figure 1). Large $\Delta\epsilon$, corresponding to high x_0 , and large ϵ_{HH} favor collapse while swollen configurations are obtained in the opposite situation. While we do not analyze the collapse transition, it is useful to note the existence of evidence that a first-order phase transition is involved.^{14,18,20,21,23–25} The configurations were first characterized via their pair correlation functions, $g_{ij}(\Delta r)$, of $i = P, H$ and $j = P, H$ monomers. These specify the probability of finding an i monomer at r' when a j monomer is located at r as a function of $\Delta r = |r' - r|$. Importantly, the three $g_{ij}(\Delta r)$ are identical for the swollen configurations but differ significantly for the collapsed ones (Figure 2). The nature of the differences is clarified by plots of the radial density $\rho_i(r)$ of monomers $i = P, H$ at a distance r from the center of mass of the chain, the overall monomer radial density $\rho(r)$ (Figure 3), and the radial distribution of the fraction of H monomers, $x(r)$ (Figure 4). For the swollen configurations, $\rho_H(r)$ and $\rho_P(r)$ are indistinguishable and $x(r)$ is constant. In marked contrast, the collapsed configurations exhibit core-shell structures. An inner dense core rich in H is surrounded by a lower density shell with a higher P fraction. Importantly, H-rich regions, characterized by local $x \approx 1$ values, are associated with high $\rho(r)$ while P-rich regions exhibit relatively low $\rho(r)$. Snapshots of the core-shell structures (Supporting Information) reveal significant shape fluctuations. As a result, $\rho_H(r)$, $\rho_P(r)$, and $x(r)$ and the overall monomer density $\rho(r)$ reflect two contributions. One is due to the density gradient along the normal to the globule surface. The second arises because of the orientational averaging of the shape fluctuations. Inspection of individual snapshots reveals dense and rather uniform globules (Figure 1, Supporting Information), thus suggesting that the shape fluctuation contributes significantly to the broadening of the exterior part of $\rho_H(r)$, $\rho_P(r)$ and $x(r)$, $\rho(r)$.

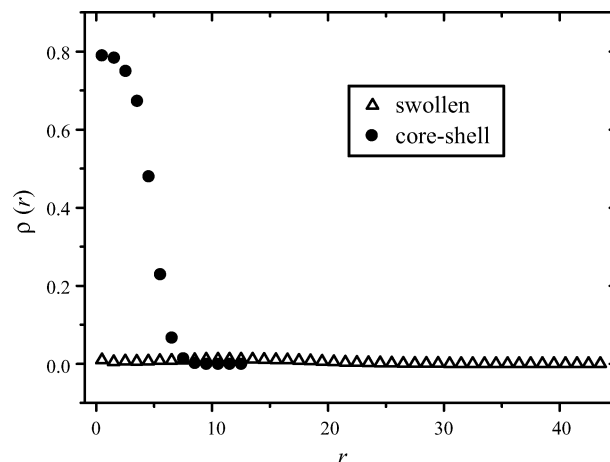


Figure 3. Overall radial monomer density, $\rho(r)$, plotted with respect to r , the distance from the center of mass for swollen chain ($\epsilon_{HH} = 1.0$, $\Delta\epsilon = -0.6$, and $x_0 = 0.089$) and a core-shell globule ($\epsilon_{HH} = 1.0$, $\Delta\epsilon = -0.2$, and $x_0 = 0.39$).

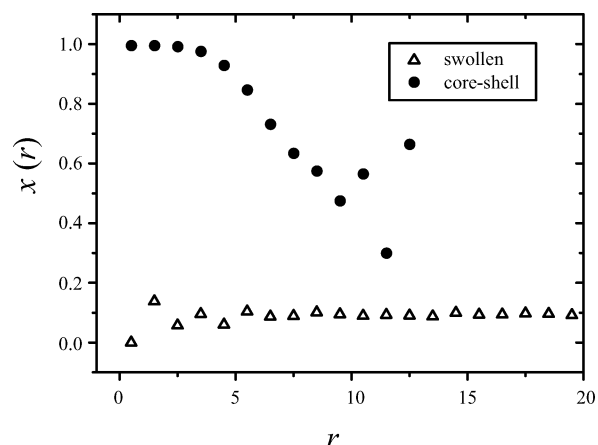


Figure 4. Radial H fraction, $x(r)$, plotted with respect to r , the distance from the center of mass for swollen chain ($\epsilon_{HH} = 1.0$, $\Delta\epsilon = -0.6$, and $x_0 = 0.089$) and a core-shell globule ($\epsilon_{HH} = 1.0$, $\Delta\epsilon = -0.2$, and $x_0 = 0.39$).

IV. Simulation Results: Distribution of States along the Chain

As we shall discuss, the dynamic core-shell structures described earlier favor the stability of globules. They arise in annealed PH copolymers comprising of interconverting solvophobic and solvophilic monomers and with no constraint on the PH ratio. The stabilization of globules can also be achieved by creating quenched core-shell structures. This direction was recently explored by Khokhlov et al.,²⁷ who pursued the design of quenched “protein-like” copolymers of hydrophobic H and hydrophilic P monomers. The first step within this in silico approach is the creation of an ensemble of collapsed homopolymer chains comprising of H monomers. The second step is the irreversible conversion of half of the H monomers, at the exterior region of the globule, into solvophilic P monomers. The outcome is an ensemble of quenched PH copolymer sequences capable of “folding” into nonaggregating globules reminiscent of proteins. While the two scenarios involve core-shell structures, the prescriptions for the creation of the sequences are different. First, the protein-like sequences are quenched while the dynamic core-shell structures involve annealed sequences. Second, the protein-like structures are obtained by converting all monomers at the exterior region to a solvophilic P state while all inner monomers remain solvophobic and a PH ratio of unity is

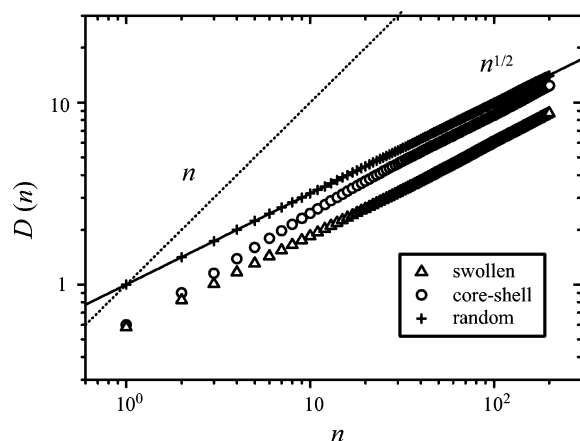


Figure 5. $\log D_n$ vs $\log n$ plots of swollen ($\Delta\epsilon = -0.6$ or $x_0 = 0.089$) and collapsed core-shell ($\Delta\epsilon = -0.2$ or $x_0 = 0.39$) configurations with $\epsilon_{HH} = 1.0$ and $N = 500$.

maintained. In the dynamic core-shell structures both the inner core and the interface comprise a mixture of P and H monomers, and there is no constraint on the PH ratio. With these differences in mind it is of interest to compare the sequences obtained in the two scenarios. To facilitate comparison, we analyze the sequences following the procedure of Khokhlov et al. The first step is the generation of a “nonrandom” walk corresponding to the HP sequence by assigning all monomers along the chain with steps $u(H) = -1$ and $u(P) = 1$. The resulting net displacement after n steps is

$$L(n) = \sum_{i=1}^n u_i \quad (5)$$

where i specifies the position of the monomer along a chain segment comprising n monomers. The correlations within the sequence are then characterized by the n dependence of the dispersion

$$D_n^2 = \sum_{i,j=k}^{k+n} (\langle u_i u_j \rangle - \langle u_i \rangle \langle u_j \rangle) \quad (6)$$

A random sequence exhibits $D_n \sim n^{1/2}$ irrespective of the interval considered while correlations are signaled by $D_n \sim n^\alpha$ with $\alpha \neq 1/2$.³⁶ Computational and analytical results concerning²⁷ the quenched protein-like sequences demonstrate two well-distinguished regimes: $\alpha \approx 1$ for small n and $\alpha \approx 1/2$ for large n limit. Three points emerge from the plots D_n vs n for the PH two-state polymers (Figure 5): (i) The swollen state of the annealed PH copolymers exhibits $\alpha \approx 1/2$ scaling corresponding to a random copolymer. (ii) The sequences associated with the dynamic core-shell structures deviate from the simple $\alpha \approx 1/2$ scaling of the swollen chains. (iii) In contrast to quenched “protein-like” copolymers, the annealed sequences corresponding to dynamic core-shell structures do not approach $\alpha \approx 1$ for small n . We will return to the first two points later, in section V. In comparing the quenched protein-like copolymers with the annealed two-state ones, it is important to bear in mind the following points. First, the PH interconversion opposes block structure in the annealed case. Second, the overall H fraction is fixed in the protein-like copolymers while it varies with the configurations in the annealed case. The overall H fraction is close to zero in the swollen configurations while it approaches unity in the core-shell case. This change is associated with a significant modification in the size distribution of the blocks

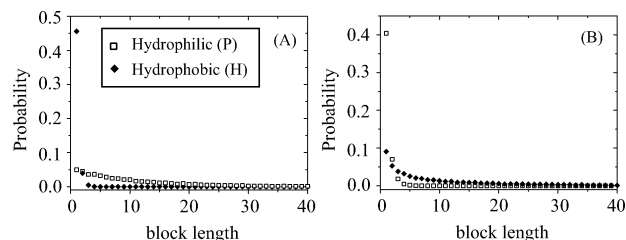


Figure 6. Probability distribution of H and P blocks as a function of the block size in swollen chains, $\Delta\epsilon = -0.2$, $x_0 = 0.089$ (A), and in core-shell configurations, $\Delta\epsilon = -0.2$, $x_0 = 0.39$ (B).

(Figure 6). In the swollen configurations the H domains are very short, comprising typically of one to two monomers, while the P blocks are much larger. The opposite trend is found in the core-shell case. It is also important to note that the sample size in the simulation study of protein-like copolymers²⁷ is larger and that the characteristics of the annealed copolymers vary somewhat with N and with the method of analysis (Supporting Information).

V. Theoretical Considerations: The H Fraction, Surface Tension, and the Role of a Fringe

The PH sequence and the configurations of the backbone are, in general, coupled. Thus, modeling the collapse of two-state polymers requires a generalization of the theory of Lifshitz and Grosberg^{26,37} (LG) to allow for the $H \rightleftharpoons P$ equilibrium and its dependence on the local monomer density and composition. This is beyond the scope of this article. Our interpretation of the simulation results and their consequences consists of two groups of simple arguments. One aims to rationalize the observed PH ratio in two limits when the PH sequences are weakly sensitive to the configurations. In particular, we will discuss highly swollen chains and the core of fully collapsed ones. The second group concerns qualitative aspects of the globules’ surface tension and interfacial structure. To this end we invoke certain conclusions of the LG theory while avoiding its detailed application.

We begin with a discussion of the H fraction x in the two “weak sensitivity” regimes where the PH distribution is largely independent of the spatial position. One is realized in good solvent conditions when the chains are swollen and the monomer concentration within them is extremely low. Consequently, monomer–monomer interactions have negligible effect on the $H \rightleftharpoons P$ equilibrium in this regime. In this situation the equilibrium distribution of PH sates approaches that of a chain of noninteracting monomers. The PH sequence may thus be modeled as an ideal one-dimensional mixture. The corresponding free energy per monomer is

$$F_0 = x\mu_H^0 + (1-x)\mu_P^0 + kT[x \ln x + (1-x) \ln(1-x)] \quad (7)$$

where μ_i^0 is the standard chemical potential of a monomer in state $i = P, H$. This free energy corresponds to the Zimm–Bragg model for the helix–coil transition^{1,38,39} in the case of zero cooperativity, $\sigma = 0$. The equilibrium condition $\partial F_0 / \partial x = 0$ yields

$$\frac{1-x_0}{x_0} = \exp\left(-\frac{\Delta\mu^0}{kT}\right) = K^0 \quad (8)$$

where $x_0 = 1/(1 + K^0)$ denotes the equilibrium H fraction in the swollen coil. Within this picture μ_i characterized the solvent quality as experienced by species i . $\Delta\mu^0 = \mu_P^0 - \mu_H^0$, as

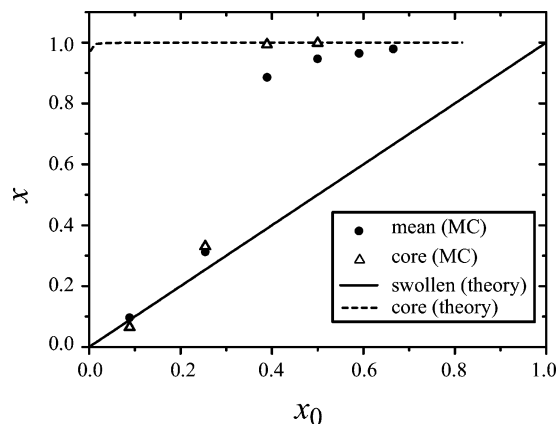


Figure 7. Comparison of the simple theory with the simulation results. Calculated $x(r=0)$ vs x_0 and calculated overall H fraction x vs x_0 with $\epsilon_{HH} = 1.0$.

determined upon comparison of (8) and (4) is

$$\frac{\Delta\mu^0}{kT} = \Delta\epsilon + \ln[2 - \exp(-\Delta\epsilon)] \quad (9)$$

The x_0 values obtained from eqs 8 and 9 agree with the simulated x values for the swollen configurations (Figure 7).

The second regime we consider concerns the globular core modeled as a dense globule of infinite size. In this case the PH sequence is insensitive to the precise chain configuration. The densely packed monomers provide “lattice sites” for the $P \rightleftharpoons H$ reaction. Because of the high monomer density within the globule, monomer–monomer interactions have a strong effect on the $H \rightleftharpoons P$ equilibrium. To characterize this equilibrium, we model the core as a dense mixture of disconnected H and P monomers inscribed on a lattice with a coordination number z and lattice constant $2^{1/6}a$. The interactions between nearest neighbors are specified by the corresponding $-\epsilon_{ij}$ of the LJ potential. The resulting free energy comprises of F_0 supplemented by an interaction energy per site, E_{core} . In turn, E_{core} as given by the Bragg–Williams approximation is

$$\frac{E_{\text{core}}}{kT} = -\frac{z}{2}[x\epsilon_{HH} + (1-x)\epsilon_{PP}] + x(1-x)\chi_{PH} \quad (10)$$

Here the first term accounts for the interaction energy as realized in two pure phases while the second is the mixing energy formulated in terms of the Flory χ parameter

$$\chi_{PH} = z \left[\frac{\epsilon_{HH} + \epsilon_{PP}}{2} - \epsilon_{PH} \right] \quad (11)$$

The equilibrium condition $\partial F_{\text{core}}/\partial x = 0$ for $F_{\text{core}} = F_0 + E_{\text{core}}$ leads to

$$\frac{1-x_c}{x_c} = \exp \left[-\frac{\Delta\mu^0}{kT} - \frac{z}{2}(\epsilon_{HH} - \epsilon_{PP}) + (1-2x_c)\chi_{PH} \right] \quad (12)$$

where x_c is the equilibrium H fraction within the core. To calculate x_c , we utilized $z = 12$ since the snapshots of the core suggest close packing. The x_c values obtained from (12) fit the observed behavior in the interior of the core as specified by the values of $x(r)$ averaged over the inner core region taken as $0 \leq r \leq 3$ (Figure 7).

This brings us to the second part of our theoretical discussion concerning the effect of the $P \rightleftharpoons H$ reaction on the surface

tension and the structure of the interface. We begin with the effect on the surface tension. To formulate a well-posed question, it is necessary to first specify a reference state involving one-state polymer. For reasons discussed below we choose a HP random copolymer with an overall H fraction identical to x_c , the H fraction in the interior of a core–shell globule, whose typical value is ≈ 0.98 . Such a copolymer may be considered as a constrained version of the annealed HP copolymer, i.e., a chain where the HP interconversion is “frozen” and a particular HP distribution is imposed. By construction, the one-state reference polymer will collapse under conditions leading to the collapse of the annealed HP copolymer. We first compare γ_1 and γ_2 denoting respectively the surface tension of globules formed by the one-state reference polymers and the annealed HP two-state polymer. A detailed theoretical analysis is required in order to obtain the numerical values of γ_1 and γ_2 . However, we limit ourselves to a much simpler argument, allowing to conclude that $\gamma_2 < \gamma_1$. To this end we recall certain features of the LG theory.^{1,26} This provides a self-consistent-field description of the globule specifying the configurations that minimize the overall free energy of the chain. In the collapsed regime the free energy of the chain comprises two terms reflecting volume and surface contributions. The interior composition of the globule is identified with the dense phase of the corresponding phase-separated system. The minimization of the free energy amounts then to minimization of the surface tension of the globule, γ . Note that γ reflects two contributions: one due to the entropy of the loops and the second arising because of monomer–monomer and monomer–solvent interactions. For one-state polymer the minimization is carried out with respect to the radial density of monomers, $\rho(r)$ in our notation. In the case of two-state polymers it is necessary to minimize this functional also with respect to $x(r)$. This additional degree of freedom implies constraint release and thus lower free energy. For our choice of reference state the volume term is not affected by the constraint release and thus $\gamma_2 \leq \gamma_1$. We now need to distinguish between $\gamma_2 < \gamma_1$ and $\gamma_2 = \gamma_1$ on the basis of the qualitative features of the simulation results. These suggest $\gamma_2 < \gamma_1$ because the configurations of the dynamic core–shell structure differ from those of the reference state. This is evident in three characteristics. First, the overall H fraction in the core shell structure, $\langle x \rangle_{\text{cs}} \approx 0.8$, differs significantly from x_c . Second, the core–shell structure is formed by nonrandom PH copolymers. Finally, the $x(r)$ profile in the dynamic core–shell globule is strongly dependent on r while $x(r) \approx \text{const}$ is expected for the reference state. Accordingly, a collapse one-state polymer in the reference state will evolve into a different state of lower free energy and lower γ corresponding to the annealed HP copolymer. This qualitative conclusion relies on the assumption the equilibrium state is independent of the initial state of the HP copolymer, i.e., its composition and sequence. In turn, this assumption is reasonable in nonglassy systems such the one explored in our simulation. Our argument is strictly applicable for the specific reference state having an overall $x = x_c$. However, it is reasonable to expect $\gamma_2 < \gamma_1$ for a family of one-state polymer with overall x at finite interval centered at x_c .

The second issue of interest concerns the structure of the globule’s interface. The LG theory of one-state polymer predicts two types of collapsed configurations: dense globules with and without a fringe. A fringe consists of dilute or semidilute loops anchored to the surface of the globule. It is a form of coexistence between dilute and concentrated monomer phases as modified by chain’s connectivity. The prediction of these two forms for

one-state polymers raises the possibility of similar structures in two-state globules. A fringe in two-state core-shell globule will have however somewhat different characteristics because it will contain a fraction of P monomers and may thus experience a better effective solvent. In our simulation the number of P monomers in the core-shell structures is smaller than the number of surface sites in a spherical globule $\sim N^{2/3}$. As discussed earlier, the P fraction in the core is very small. We can thus envision two scenarios: (i) a fringless globule where most of the P monomers are located at a dense HP monolayer at the globules's interface and (ii) a fringed globule with few P monomers embedded at the core's interface and the rest forming solvent swollen loops anchored to the surface. It is difficult to distinguish between these two possibilities on the basis of the simulation results because of the shape fluctuations of the globule. Since a detailed theoretical analysis is beyond the scope of this article we resort to a heuristic argument favoring the fringed globule picture. This argument is indirect because it does not allow to compare the free energies of the two states. It can only suggest that the dense monolayer scenario is unattainable. To this end we consider a dense globule with a majority of H with an exterior shell comprising a binary mixture monolayer of P and H. Two ingredients distinguish such a shell from the dense core: (i) One is the missing exterior neighbors. Within this simplified model, the interfacial layer experiences interactions with the dense H core substrate. The next layer, at higher distance r from the center, is vacant. As a result, the interaction energy now involves a smaller number of neighbors. (ii) The second ingredient is the possibility of incomplete occupation of the interfacial layer. A fraction $Y \leq 1$ of the surface sites is occupied, thus affecting both the mixing entropy and the interactions. We accordingly consider the interfacial layer as a ternary mixture inscribed on a two-dimensional lattice with coordination number z_s . $1 - Y$ of the sites are vacant and do not contribute to the interaction energy. Of the remaining sites, the fraction occupied by H is Yx_s while that occupied by P is $Y(1 - x_s)$. Within our simple argument Y is an adjustable parameter. The counterpart of F_0 is thus

$$\tilde{F}_0 = Y[x_s\mu_H^0 + (1 - x_s)\mu_P^0] + kT[1 - Y]\ln(1 - Y) + Y\ln Y + Yx_s\ln x_s + Y(1 - x_s)\ln(1 - x_s) \quad (13)$$

This free energy does not allow for loop entropy. Since it corresponds to scenario i, there are no loops swollen by the solvent. Loops oriented toward the core give rise to a constant term because their statistics are independent of the P fraction at the interface. The interaction free energy of the shell, within the Bragg-Williams approximation, is

$$\frac{E_{\text{shell}}}{kT} = -\frac{z_s}{2}Y^2[x_s\epsilon_{HH} + (1 - x_s)\epsilon_{PP}] + Y^2x_s(1 - x_s)\frac{z_s}{z}\chi_{PH} - \frac{z - z_s}{4}Y[x_s\epsilon_{HH} + (1 - x_s)\epsilon_{PH}] \quad (14)$$

The first two terms account for the in-plane interaction energy of the two-dimensional lattice mixture. $(z_s/z)\chi_{PH}$ replaces χ_{PH} to allow for the lower coordination number. However, each interfacial particle is embedded in the three-dimensional lattice with coordination number z . Of these z neighbors, the external $(z - z_s)/2$ are vacant and do not give rise to interactions. The inner $(z - z_s)/2$ neighbors are interior core H monomers. Since we only consider the interaction energy at the interface, the pair interaction energies ϵ_{ij} are replaced by $\epsilon_{ij}/2$ to avoid double counting. The equilibrium condition $\partial F_{\text{shell}}/\partial x_s = 0$ for $F_{\text{shell}} =$

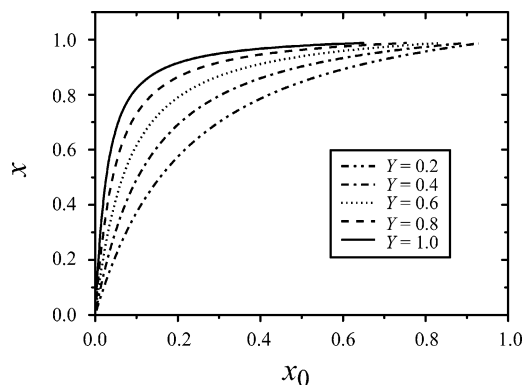


Figure 8. Plots of x_s vs x_0 for $\epsilon_{HH} = 1.0$ and different Y values.

$\tilde{F}_0 + E_{\text{shell}}$ specifies the equilibrium H fraction in the shell, x_s

$$\frac{1 - x_s}{x_s} = \exp\left[-\frac{\Delta\mu^0}{kT} - Y\frac{z_s}{2}(\epsilon_{HH} - \epsilon_{PP}) + Y(1 - 2x_s)\frac{z_s}{z}\chi_{PH} - \frac{z - z_s}{4}(\epsilon_{HH} - \epsilon_{PH})\right] \quad (15)$$

Having chosen $z = 12$ to characterize the dense core, we assume $z_s = 6$ for the surface layer. Equation 15 demonstrates that low x_s values are only possible for low Y (Figure 8). This indicates that a dense P-rich shell coating an H-rich core is unfavorable. A P-rich shell requires low Y , suggesting instead a fringed shell. Within such a fringe the $P \rightleftharpoons H$ equilibrium in the loops is dominated by $\Delta\mu^0$, thus permitting a P-rich shell.

VI. Discussion

Our simulation of a minimal two-state polymer model provides evidence for the occurrence of dynamic core-shell globules having a solvophobic interior and solvophilic exterior. The PH sequence associated with these collapsed configurations exhibits correlations, in contrast to the random sequence in the swollen coils. These correlations are however weaker in comparison to those characterizing quenched "protein-like" PH copolymers that yield somewhat similar core-shell structures. The surface tension associated with such dynamic core-shell globules is expected to be lower than that of a corresponding one-state globules. In turn, this modifies the phase diagram by decreasing the driving force for globule aggregation. This provides a possible route for reconciling the observation of thermodynamically stable dilute solutions of dense PNIPAM globules with theory. The reduced surface tension of dense two-state polymers may also be relevant to the discussion of the formation of stable "mesoglobules" by other NWSP. Other stabilization mechanisms were proposed to rationalize these effects. These invoke effects of vitrification, reptation, and viscoelasticity.⁴ Importantly, these mechanisms are equally operational for neutral homopolymers in organic solvents and in water. In other words, they apply to both one-state and two-state polymers. In contrast, the mechanism proposed above is limited to polymers exhibiting two-state behavior such as NWSP in aqueous solutions. It is of special interest because the observations of stable globules and mesoglobules appear, at present, to be a characteristic of these systems.

Theories concerning the collapse of annealed two-state models emerged, independently, from considerations concerning NWSP^{14,18,23,40} and of biopolymers.^{20,21,24,25} The essential physics of these models are similar, but the relationship between them was obscured by the different systems considered. All approaches predict the possibility of collapse via first-order

phase transition. The work on biopolymers is however of special interest since it discusses also the possibility of phase separation within the globule.^{20,24,25} The two-state polymers envisioned were biopolymers undergoing a helix–coil transition or chains with monomers capable of complexation of ligands. It is useful to note that the first case involves a unimolecular reaction similar to the $P \rightleftharpoons H$ interconversion we consider. In contrast, the second scenario concerns a bimolecular reaction between the monomers and the ligands. Early work²⁴ focused on the coupling of the helix–coil and the collapse. It predicted a first-order collapse transition leading to phase-separated globules whose possible morphologies include concentric spheres, a globule attached to a coil, and a dumbbell. The precise morphology was not specified. The possibility of a first-order collapse transition associated with a core–shell structure was later discussed by Garel et al.²⁰ A more recent work²⁵ studied the first-order phase collapse transition allowing for intrachain phase separation. It focused on the concentric sphere morphology and utilized a simplified approach based on a Flory-type free energy. In both^{20,25} the PH sequence is annealed, but the overall fraction of H monomers is constrained and does not change upon collapse. This constrained annealing assumption rules out comparison to our system where the annealing is free of constraints and the overall H fraction changes with the swelling degree. The discussions cited above did not address the surface tension of the two-state globule and its possible effect on the phase diagram. In the introduction and in section IV we have discussed quenched “design” protein-like PH copolymers where the H to P conversion was carried out irreversibly and in a single step.²⁷ It is of interest to comment on the related evolutionary design procedure where partial PH annealing occurs.^{32b} Within this simulation the sequence evolves via an iterative procedure. In one step the sequence undergoes PH conversion, “mutations”, retaining sequences satisfying the Metropolis criterion. In the second, the chain configuration is partially reequilibrated. Importantly, the mutation steps are short (1 MC step) and involve only a fraction of the monomers (10%) while all monomers participate in the long (10^4 MC steps) configuration relaxation step. Furthermore, in this simulation the MC updates for the sequence and for the configurations can involve different temperatures T_{seq} and T_{conf} . Our simulation differs in two respects: (a) there is no intentional introduction of $T_{\text{conf}} \neq T_{\text{seq}}$, and (b) the updates of the sequence and the configuration occur simultaneously and both involve all monomers. Under these conditions we expect the heat flow between the configuration and sequence to ensure $T_{\text{conf}} = T_{\text{seq}}$. Our case is thus closest to the “annealed case”, $T_{\text{conf}} = T_{\text{seq}}$, of Chertovich et al.^{32b} However, the two differ because Chertovich et al. impose a constraint requiring a 1:1 PH ratio while our system allows the PH ratio to vary.

As noted previously, two-state models were developed for two families of polymers. One is NWSP in water. The second comprises biopolymers such as heliogenic polypeptides and nucleic acids as well as biopolymers binding ligands such as dyes, metal ions, etc. Our minimal model and the associated simple theory are clearly oriented toward NWSP in water. Importantly, the experimental situation concerning these two families of polymers is different. In the case of heliogenic biopolymers there is direct structural and spectroscopic evidence for the two states. The evidence for the two states of NWSP is indirect. As we shall discuss, this influences the choice of future research in this area. It is first useful to comment on the experimental support for two-state models. As discussed previously, the important merit of two-state models is their ability

to rationalize the phase diagram of NWSP, in particular their insolubility loop. The distinctive collapse behavior of NWSP in water may be considered as additional support for the two-state models of such polymers. In addition, the two-state hypothesis of PNIPAM also allows to rationalize features of the collapse of PNIPAM brushes. A two-state model for PNIPAM was first suggested for PNIPAM brushes by Zhu and Napper,⁴⁰ who interpreted their experimental results in terms of a vertical phase separation within a PNIPAM brush. Such vertical phase separation is a form of core–shell structure. It involves a first-order phase transition leading to an exterior hydrophilic layer and an inner hydrophobic one. The possibility of such vertical phase separation was first discussed by Wagner et al.¹⁷ within the n -cluster model proposed by de Gennes.¹⁶ It is however a general property of two brushes formed by two-state polymers.⁴¹ Two qualitative experimental observations support this scenario. First is an early study by Zhu and Napper⁴⁰ of the collapse of PNIPAM brushes grafted to latex particles immersed in water. This revealed a collapse involving two stages. An “early collapse” took place below 30 °C, at better than “ θ conditions”, and did not result in flocculation of the neutral particles. Upon raising the temperature to worse than “ θ conditions” the collapse induced flocculation. This indicates that the colloidal stabilization imparted by the PNIPAM brushes survives the early collapse. It led to the interpretation of the effect in terms of a vertical phase separation within the brush due to a second type of phase separation as predicted by the n -cluster model. More recently, Balamurugan et al.⁴² used surface plasmon resonance (SPR) and contact angle measurements with water to characterize PNIPAM brushes “grafted from” a self-assembled monolayer on gold. The brush properties were studied at between 10 and 40 °C. The SPR measurements indicated gradual variation of the brush properties. In marked contrast, the contact angle measurements revealed an abrupt change at ~ 32 °C. Recent experiments utilizing neutron reflectometry⁴³ and surface force measurements⁴⁴ also lend support to the vertical phase separation scenario.

The indirect experimental support for the validity of two-state models does not currently enable to determine the nature of the interconverting states. Similarly, a technique to monitor their relative weight and spatial distribution has not yet emerged. Clearly, the minimal model investigated in this work cannot capture the full complexity of NWSP in water. On the other hand, study of hydration and its coupling to the local water structure requires all-atom simulation with explicit water molecules as performed for PEO. For PNIPAM, with its greater complexity, this is a demanding task. With these points in mind it is of interest to further investigate minimal models with view of answering two questions. First, how sensitive is the dynamic core–shell globule to the details of the model? Second, are these structures associated with distinctive signatures detectable by scattering techniques?

Acknowledgment. N.Y. benefited from fellowship No. 1142 from the Japan Society for the Promotion of Science (JSPS) as well as support from Commissariat à l'énergie atomique–Grenoble while visiting Grenoble. Numerical computations reported in this work were partly carried out at the Yukawa Institute Computer Facility.

Supporting Information Available: Snapshots of the core–shell structures; sequence analysis. This material is available free of charge via the Internet at <http://pubs.acs.org>.

References and Notes

- (1) Grosberg, A. Yu.; Khokhlov, A. R. *Statistical Physics of Macromolecules*; American Institute of Physics: New York, 1994.
- (2) Baysal, B. M.; Karasz, F. E. *Macromol. Theory Simul.* **2003**, *12*, 627–646.
- (3) Williams, C.; Brochard, F.; Frich, C. H. *Annu. Rev. Phys. Chem.* **1981**, *32*, 433–451.
- (4) Aseyev, V. O.; Tenhu, H.; Winnik, F. *Adv. Polym. Sci.* **2006**, *196*, 1–85.
- (5) Timoshenko, E. G.; Koznetsov, Yu. A. *J. Chem. Phys.* **2000**, *112*, 8163–8175.
- (6) Wu, C.; Wang, X. *Phys. Rev. Lett.* **1998**, *80*, 4092–4094.
- (7) Wang, X.; Qiu, X.; Wu, C. *Macromolecules* **1998**, *31*, 2972–2976.
- (8) Wu, C.; Zhou, S. *Macromolecules* **1995**, *28*, 8381–8387.
- (9) Zhang, G.; Wu, C. *Adv. Polym. Sci.* **2006**, *195*, 101–176.
- (10) Goldstein, R. *J. Chem. Phys.* **1984**, *80*, 5340–5341.
- (11) Karlström, G. *J. Phys. Chem.* **1985**, *89*, 4962–4964.
- (12) Matsuyama, A.; Tanaka, F. *Phys. Rev. Lett.* **1990**, *65*, 341–344.
- (13) Dormidontova, E. *Macromolecules* **2002**, *35*, 987–1001.
- (14) Jeppesen, C.; Kremer, K. *Eurphys. Lett.* **1996**, *34*, 563–568.
- (15) Veytsman, B. A. *J. Phys. Chem.* **1990**, *94*, 8499–8500.
- (16) de Gennes, P. G. *C. R. Acad. Sci., Ser. II* **1991**, *313*, 1117–1122.
- (17) Wagner, M.; Brochard, Wyart, F.; Hervet, H.; de Gennes, P. G. *Colloid Polym. Sci.* **1993**, *271*, 621–628.
- (18) Bekiranov, S.; Bruinsma, R.; Pincus, P. *Europhys. Lett.* **1993**, *24*, 183–188.
- (19) Bekiranov, S.; Bruinsma, R.; Pincus, P. *Phys. Rev. E* **1997**, *55*, 577–585.
- (20) Garel, T.; Leibler, L.; Orland, H. *J. Phys. II* **1994**, *4*, 2139–2148.
- (21) Trovato, A.; van Mourik, J.; Maritan, A. *Eur. Phys. J. B* **1998**, *6*, 63–73.
- (22) Mattice, W. L.; Misra, S.; Napper, D. H. *Europhys. Lett.* **1994**, *19*, 603–608.
- (23) Baulin, V. A.; Halperin, A. *Macromol. Theory Simul.* **2003**, *12*, 549–559.
- (24) Grosberg, A. Y. *Biofizika* **1984** *29*, 569–573 (*Biophysics* **1984**, *29*, 621–626).
- (25) Dormidontova, E. E.; Grosberg, A. Y.; Khokhlov, A. R. *Macromol. Theory Simul.* **1992**, *1*, 375–385.
- (26) Lifshitz, I. M.; Grosberg, A. Y. *Sov. Phys. JETP* **1974**, *38*, 1198–1208.
- (27) (a) Khokhlov, A. R.; Khalatur, P. G. *Phys. Rev. Lett.* **1999**, *82*, 3456–3459. (b) Zheligovskaya, E. A.; Khalatur, P. G.; Khokhlov, A. R. *Phys. Rev. E* **1999**, *59*, 3071–3078. (c) Govorun, E. N.; Ivanov, V. A.; Khokhlov, A. R.; Khalatur, P. G.; Borovinsky, A. L.; Grosberg, A. Y. *Phys. Rev. E* **2001**, *64*, 040903. (d) Khalatur, P. G.; Khokhlov, A. R. *Adv. Polym. Sci.* **2006**, *195*, 1–100.
- (28) The positions of the phase boundaries with respect to the boiling and freezing temperatures of water determine the observed phase diagram.
- (29) (a) Smith, G.; Bedrov, D. *Macromolecules* **2002**, *35*, 5712–5719. (b) Smith, G.; Bedrov, D. *J. Phys. Chem. B* **2003**, *107*, 3095–3097. (c) Smith, G.; Bedrov, D.; Bedrov, D.; Borodin, O. *J. Am. Chem. Soc.* **2000**, *122*, 9548–9549. (d) Smith, G.; Bedrov, D.; Borodin, O. *Phys. Rev. Lett.* **2000**, *85*, 5583–5586.
- (30) Tasaki, K. *J. Am. Chem. Soc.* **1996**, *118*, 8459–8469.
- (31) Heymann, B.; Grubmüller, H. *Chem. Phys. Lett.* **1999**, *307*, 425–432.
- (32) (a) Khalatur, P. G.; Novikov, V. V.; Khokhlov, A. R. *Phys. Rev. E* **2003**, *67*, 051901. (b) Chertovich, A. V.; Govorun, E. N.; Ivanov, V. A.; Khalatur, P. G.; Khokhlov, A. R. *Eur. Phys. J. E* **2004**, *13*, 15–25.
- (33) Baulin, V.; Halperin, A. *Macromolecules* **2002**, *35*, 6432–6438.
- (34) Chu, B.; Ying, Q. C.; Grosberg, A. Y. *Macromolecules* **1995**, *28*, 180–189.
- (35) Baumgärtner, A. *J. Chem. Phys.* **1980**, *72*, 871–879.
- (36) Bouchaud, J. P.; Georges, A. *Phys. Rep.* **1990**, *195*, 127–293.
- (37) Lifshitz, I. M.; Grosberg, A. Y.; Khokhlov, A. R. *Rev. Mod. Phys.* **1978**, *50*, 683–713.
- (38) Zimm, B. H.; Brag, I. K. *J. Chem. Phys.* **1959**, *31*, 526–535.
- (39) Buhot, A.; Halperin, A. *Phys. Rev. Lett.* **2000**, *84*, 2160–2163.
- (40) (a) Zhu, P. W.; Napper, D. H. *J. Colloid Interface Sci.* **1994**, *164*, 489–494. (b) Zhu, P. W.; Napper, D. H. *Colloid Surf., A* **1996**, *113*, 145–153.
- (41) Baulin, V. A.; Zhulina, E. B.; Halperin, A. *J. Chem. Phys.* **2003**, *119*, 10977–10988.
- (42) Balamurugan, S.; Mendez, S.; Balamurugan, S. S.; O'Brien II, M. J.; Lopez, G. P. *Langmuir* **2003**, *19*, 2545–2549.
- (43) Yim, H.; Kent, M. S.; Satija, S.; Mendez, S.; Balamurugan, S. S.; Balamurugan, S.; Lopez, G. P. *Phys. Rev. E* **2005**, *72*, 051801.
- (44) Plunkett, K. N.; Zhu, X.; Moore, J. S.; Leckband, D. E. *Langmuir* **2006**, *22*, 4259–4266.

MA0622090